ORIGINAL SCIENTIFIC PAPER OPEN ACCESS

Effect of welding electrode variation on microstructure and mechanical properties of AISI 204 stainless steel plates joined using shielded metal arc welding

Henry Ekene Mgbemere[1], Chiedozie Valentine Oluigbo[2*]

[1] University of Lagos, Department of Metallurgical and Materials Engineering, Lagos State, Nigeria.

[2] Federal Polytechnic Ilaro, Department of Welding and Fabrication Engineering Technology, Ogun State, Nigeria

ARTICLE INFO

[*] **Correspondence:** olu7wonders@yahoo.com

DOI: 10.5937/engtoday2400002M

UDC: 621(497.11) **ISSN:** 2812-9474

Article history: Received 1 November 2023; Revised 9 January 2024; Accepted 15 January 2024

ABSTRACT

The current study investigates the effect of some welding electrodes and post-weld heat treatment on the microstructure, tensile strength, and hardness of austenitic stainless steel (AISI 204) weldments using the shielded metal arc welding (SMAW) technique. Four different electrode specifications were used in this study, these include stainless steel electrodes (E308L and E308L-16) and mild steel electrodes (E6013 and E7018). Samples of the austenitic stainless-steel plate of 5 mm thickness were first sectioned and welded across the width using the four electrodes. Following the welding operations, a post-weld heat treatment was carried out at 1100°C, soaked for 60 minutes, and then allowed to cool naturally in the open air. Both the heat-treated and the as-welded samples were then subjected to tensile and hardness tests. The hardness and ultimate tensile strength of the weldments with mild steel electrodes are higher than those of stainless-steel electrodes. However, heat treatment after the welding results in even higher hardness and ultimate tensile strength values for all the weldments except for the E6013 electrode. It is, therefore, not advisable to use inappropriate electrodes to weld austenitic stainless steel. Also, the high difference in mechanical properties between the weldments and the base metal will introduce stresses to the material, resulting in solidification cracking. The microstructures of the weldments show distinct dark and bright features, which indicates the depletion of elements like Cr in the steel.

KEYWORDS

Electrodes, Heat treatment, Mechanical properties, Microstructure, Shielded metal arc welding, Stainless steel

1. INTRODUCTION

Welding is often considered the most cost-effective and efficient method for permanently joining metallic materials [1]. Shielded Metal Arc Welding (SMAW) is widely recognised as a fast and adaptable welding technique, particularly for its effectiveness in welding stainless steel [2]. This technique is particularly advantageous when combining intricate geometries that pose challenges for automated welding procedures. The process is notable for the utilisation of coated solid electrode wire [3]. SMAW, also called manual metal arc welding (MMAW), employs the thermal energy generated by an electric arc formed between a consumable electrode coated with flux and the workpiece to combine metallic materials [4]. Carefully selecting an electrode during the welding process is a crucial and pivotal stage in ensuring desirable weld joint qualities. The selection of electrodes is primarily influenced by two key factors: the types

© Faculty of Mechanical and Civil Engineering in Kraljevo. All rights reserved

of base material and the prevailing service conditions [5]. Stainless steels possess numerous advantageous properties that can be effectively utilised in various construction applications [6]. The AISI 204 is an austenitic stainless steel that falls under the 200 series, specifically the chromium-manganese-nitrogen series. The inclusion of nitrogen in stainless steel grades, particularly those that contain manganese, offers numerous benefits. These include enhanced strength, decreased dependence on nickel to maintain the austenite structure, decreased precipitation tendencies due to nitrogen's higher solid solubility than carbon, and added strength developed through cold deformation. Furthermore, nitrogen enhances the resistance of these steels to stress corrosion cracking (SCC). This particular kind of stainless steel is commonly employed in a variety of general applications, as well as in the fabrication of pressure vessels that are exposed to elevated temperatures and moisture [7].

Various studies have investigated the effect of electrodes on the properties of welded components. Tahir *et al.* [8] examined the mechanical properties of joints made from AISI 1020 low-carbon steel using the SMAW process. The researchers investigated the effects of various electrodes, namely E6013, E7016, and E7018, and varied current levels of 80A and 90A. The findings demonstrate that the tensile strength and hardness of the welded metal are significantly influenced by the types of welding electrodes and current levels employed.

Abdel-Wanees *et al.* [9] investigated the microstructural and mechanical properties of AISI 304 austenitic stainless-steel plates welded using SMAW with two distinct electrodes (E308L-16 and E312-17). The AISI 304 steel specimens welded using E308L-16 electrodes exhibit lower joint efficiency, increased elongation, and higher hardness than specimens welded with E312-17 electrodes.

Vashishtha *et al.* [10] conducted a study to investigate the effect of electrodes (E308, E309, and E310) on the microstructure and mechanical properties of ultra-low nickel austenitic stainless-steel joints welded using the SMAW process. The study's findings revealed that E308 displays greater hardness and tensile strength, whereas E310 exhibits higher impact strength.

The study conducted by Magudeeswaran *et al.* [11] examined the effects of different welding electrodes on the tensile and impact properties of SMAW weldments made from quenched and tempered AISI 4340 grade steel. The joints made using low hydrogen ferritic (LHF) steel electrodes exhibited superior transverse tensile characteristics compared to the other joints. The impact properties of the joints produced using high nickel steel (HNS) electrodes were found to be superior compared to the impact properties of other joints.

Mosaad and Mohamed [12] investigated the effect of electrode type (E316L-16 and E312-17) on the properties of AISI 316 austenitic stainless-steel plates joined using SMAW. The study's findings indicate that the specimens of AISI 316 stainless steel, which were welded using E316L-16 electrodes, demonstrated a greater joint efficiency than those welded using E312-17 electrodes. Further studies by [5][13][14] also highlighted the significance of electrode selection in obtaining the required mechanical properties of welded joints.

Therefore, this work investigates the effect of welding austenitic stainless steel (AISI 204) using SMAW with different electrodes on the microstructure and some mechanical properties. An extensive study of AISI 204 plates joined using SMAW will contribute to the establishment of a comprehensive knowledge base. This information will effectively guide individuals in using this welding technique, using appropriate electrodes, to achieve defect-free welds and enhance joint characteristics with greater efficiency.

2. MATERIALS AND METHODS

2.1. Chemical Analysis

The base metal used for this study is AISI 204, purchased from Owode Onirin in Lagos State, Nigeria. An optical emission spectrometer test was carried out to determine the composition of the stainless steel. A spark discharge was used to excite the atoms and ions in the steel into emission of radiation. The radiation emitted was passed to the spectrometer through an optical fibre dispersed into its spectral components. Each element has a specific wavelength, and the most suitable line for the application was measured using the photomultiplier. The radiation intensity proportional to the concentration of the element in the sample was calculated internally from a stored set of calibration curves. It was shown directly as the percentage concentration for each element. The base metal was prepared by sectioning them very slowly and carefully to minimize any heat generated during sample cutting, as this would alter the stainless steel microstructure. The shielded metal arc welding parameters used in this study include welding current of 110 A, welding speed of 60 mm/min, voltage of 40 V, and DC electrode negative. The test coupons were welded with four electrodes to form a single v-groove weld. The SMAW method employed used the following types of electrodes: E308L, E308L-16, E6013, and E7018. The chemical compositions of these welding electrodes are shown in Table 1. E308L and E308L-16 are stainless steel-coated electrodes, while E6013 and E7018 are mild steel-coated electrodes.

Table 1: Table showing the elemental composition of the different welding electrodes

Elements (wt.%)	C	Mn	Si	Cr	Ni	S	P	Mo	Cu	V
E 308L	0.04	1	1	20	10	0.03	0.04	0.75	0.75	-
E 308L-16	0.03	1	0.9	20	10	0.03	0.04	0.75	0.75	-
E 6013	0.08	0.39	0.25	0.04	0.04	0.016	0.012	0.01	-	0.01
E 7018	0.05	0.93	0.38	0.05	0.04	0.009	0.012	0.01	-	0.01

2.2. Tensile and Hardness Testing

Using the lathe machine, samples for tensile characterisation were prepared by machining them longitudinally along the weld joint into a dog-bone rectangular cross-section shape. The samples were placed in a universal tensile machine, and the load was gradually applied in tension until they fractured. A Brinell hardness tester was used with a 10 mm spherical indenter for the hardness measurement. The hardness evaluation was conducted longitudinally along the weld joint. A fixed load of approximately 6.8 kN was applied to the samples for 5 mins. The indentation diameter was measured and used to calculate the hardness value on completion of the process. The welded samples were heat-treated to 1100°C, held for 1 h, and then allowed to cool naturally in the open air, after which the hardness and tensile strength of the samples were re-measured. The hardness tests were conducted at three points on each sample, and the average values were recorded.

2.3. Scanning Electron Microscopy (SEM)

The welded samples were cut and mounted with a polymer to prepare them for microstructural examination. Coarse grinding was done with SiC abrasive paper ranging from 240 µm to 1000 µm. The first polishing stage used a nylon cloth-covered electrically powered disk. The polishing of the samples began with 25 µm aluminum oxide particles suspended in water, and the final surface grinding layer was removed entirely. Subsequently, the 5 µm stage was carried out, followed by the final polishing stage using a 1 µm aluminium oxide suspension, which resulted in a mirror-like surface free of scratches. Chemical etching was done on the samples using picric acid, hydrochloric acid, and ethanol.

3. RESULTS AND DISCUSSION

3.1. Chemical Analysis

The steel's composition was determined using X-ray fluorescence examination, revealing that it corresponds to AISI 204, as indicated in Table 2. The main alloying elements that make steel austenitic stainless steel are Nickel and Chromium. However, Ni in the AISI 204 was reduced to 0.6 wt. % while the amount of Mn was increased to 8.8 wt. %. In the case of the 200 series austenitic stainless steels, manganese is the main austenite stabilizer instead of nickel, with a wt. % of 8.793 Mn.

Table 2: Elemental composition analysis of the 204 austenitic stainless steel

Element	Fe	C	Si	Mn	P	S	Cr
Amount (wt.%)	73.02 ± 0.235	0.145 ± 0.0169	0.112 ± 0.0463	8.793 ± 0.0821	> 0.07 ± 0.0066	0.0095 ± 0.0023	13.81 ± 0.2472
Element	**Ni**	**Mo**	**Cu**	**Nb**	**Co**	**V**	**W**
Amount (wt.%)	0.5554 ± 0.0142	<0.003	1.833 ± 0.1345	0.5808 ± 0.055	0.0288 ± 0.0023	0.0606 ± 0.0044	0.8708 ± 0.0217

The carbon content in stainless steel is usually maintained at a low level due to the risk of reactivity with chromium at elevated temperatures, resulting in the formation of $Cr_{23}C_6$ precipitates. This process results in a significant depletion in chromium content along the grain boundaries of the stainless steel, causing sensitization and, subsequently, intergranular corrosion. A high difference in stress between the base metal and the weldment leads to stress corrosion cracking. The weldments should have low residual stresses, a similar hardness value to the base metal, and, most importantly, no pearlite or carbide precipitation in the weldments.

3.2. Tensile Analysis

A typical E6013 electrode alone in the as-welded condition has an Ultimate Tensile Strength (UTS) of 514 MPa, yield strength of 463 MPa, and the percentage elongation in 50 mm is 30%. An E7018 electrode has a UTS value of 529 MPa, yield strength of 441 MPa, and a percentage elongation in 50 mm is 32%. The typical values for the E308L electrode are UTS of 593 MPa, yield strength of 207 MPa, and the percentage elongation in 50 mm is 48%. For the E308L-16 electrode, the UTS is 595 MPa, yield strength of 420 MPa, and the percentage elongation in 50 mm is 40% [15].

The tensile test result for the weldments as a function of the type of electrode used for welding is depicted in Figure 1. The figure shows the graph of ultimate tensile strength and percentage elongation as a function of the electrode type used for welding. The Percentage elongation values of the weldments were all lower than those of the electrodes. The percent elongation of the welded joint with the lowest carbon content (E308L-16 electrode) is the highest (16.8 %), followed by the E7018 electrode with an elongation of 14.8 %. The welded sample with the lowest elongation (13 %) is from the E6013 electrode. The stainless steel electrodes obtained the lowest UTS values (331 MPa for E308L electrodes and 354 MPa for E308L–16 electrodes). The mild steel electrodes, on the other hand, have UTS values of 676 MPa for the E6013 electrode and 453 MPa for the E7018 electrode. The type 204 stainless steel has a UTS value of 204 MPa, similar to the strength value of the weldments with stainless steel electrodes.

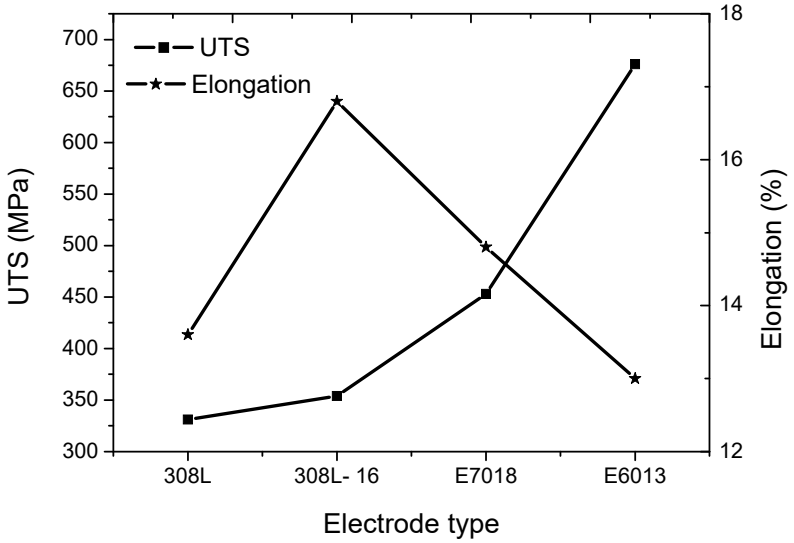

Figure 1: A graph of Ultimate Tensile Strength (UTS) and percentage elongation as a function of the welding electrode used in the stainless steel weldments

The result of the Brinell hardness test is shown in Table 3. The mild steel welding electrodes have higher values than the stainless steel electrodes. BHN values of 202 and 138 were obtained for weldments with E6013 and E 7018 electrodes, respectively, while BHN 90 and 91 were obtained for weldments with E308L-16 and E308L electrodes, respectively. The weldments with mild steel electrodes have higher hardness values than the base metal. This will induce an unevenly distributed stress to the material, which may lead to cracking. The welded samples were heat-treated to ensure the stress distribution was even.

Table 3: Hardness values (BHN) for the steel weldments carried out with different welding electrodes

S/N	Description of Sample	Hardness (BHN)
1	E308L	91
2	E308L - 16	90
3	E6013	202
4	E7018	138

3.3. Mechanical Properties after Heat Treatment

Table 4 shows the results of the hardness and ultimate tensile strength values of the weldments before and after heat treatment. The samples were heat-treated at 1,100°C for 1 h, and the hardness values after heat treatment showed an increment for weldments with stainless steel electrodes.

The hardness value for the weldment with type E308L electrode significantly increased to 191 BHN from 91 BHN, while that for type E308L -16 electrode increased from 90 to 126 BHN. The possible reason for the increase in hardness

value is the formation of chromium carbides, which makes them susceptible to stress corrosion cracking. For the non-stainless steel electrodes, the hardness values of the weldments produced using the E6013 electrode decreased from 202 to 126 BHN, while that for weldment with the E7018 electrode increased from 138 to 199 BHN. The ultimate tensile strength values for the weldments increased except for weldment with the E6013 electrode. The weldment with stainless steel electrode E308L significantly increased from 331 to 660 MPa, while weldment with E308L-16 electrode increased to 433 MPa from 354 MPa. The weldment with the E7018 electrode rose from 453 to 686 MPa. The implication is that the difference in strength values between the samples before and after heat treatment increases, which will most likely lead to higher stresses between the areas close to the welded joint and the base metal.

Table 4: Table showing the hardness and ultimate tensile strength values of the samples before and after heat treatment

Electrode Type	**Hardness** (before heat treatment)	**Hardness** (after heat treatment)	**UTS** (before heat treatment)	**UTS** (after heat treatment)
E308L	91	191	331	660
E308L -16	90	126	354	433
E6013	202	126	676	434
E7018	138	199	453	686

3.4. Microstructural Examination

The electron micrograph of the weldment, optical micrographs of the base metal, heat affected zone, fusion zone, and the microstructure of the sample showing the spots where the energy dispersive spectroscopy (EDS) analyses were carried out are shown in Figure 2. Some weld defects are observed on the surface of the weld, while the grains are not visible on the base metal. The grains are well formed at the heat-affected zone and are partially formed at the fusion zone. Dark and bright features can be seen on the microstructure, and to understand why they are so, EDS was carried out at different positions. Table 3 shows the elemental distribution of the marked positions for the weldment with the E308L electrode. The dark features on the micrograph correspond to positions 3, 6, and 7.

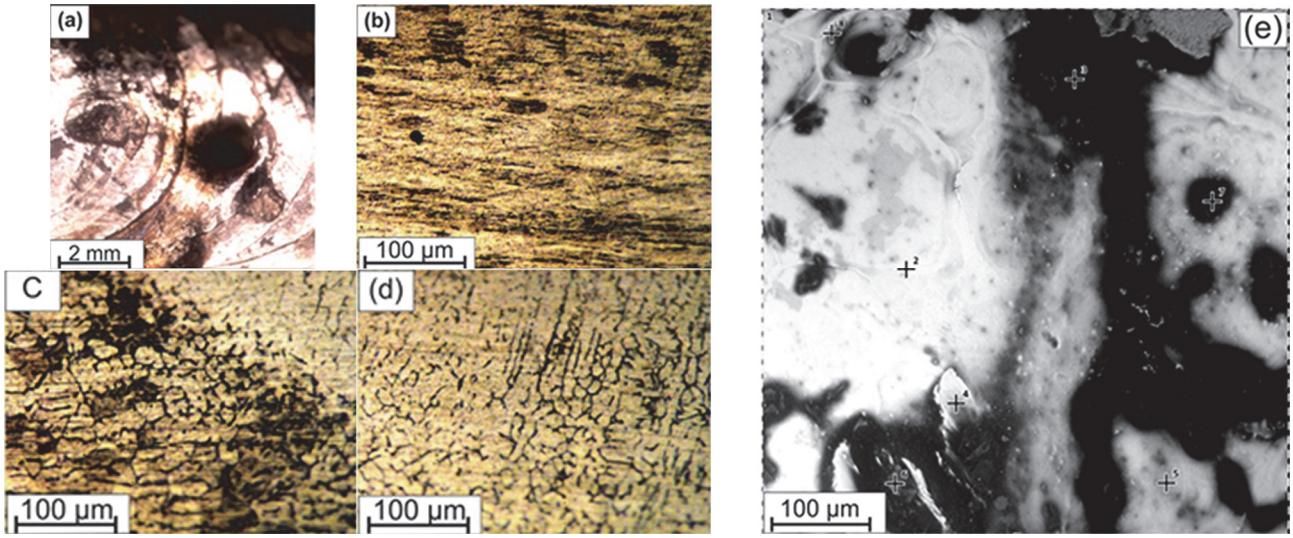

Figure 2: (a) Scanning electron micrograph of the welded joint using stainless steel E308L -16 electrode (b) Optical micrograph of the base metal with a magnification of X200 (c) Heat Affected Zone of the E308L-16 electrode weldments with a magnification of X200 (d) the fusion zone of the E308L-16 electrode weldments with a magnification of X200 and (e) Micrograph of the welded joint with E308L -16 electrode showing the spots where EDS analysis was carried out

In the weldment with an E308L-16 electrode, one common feature is that Cr is depleted while the iron content is low. An explanation could be that a new phase is formed in this region, which depletes the Cr and Fe in these positions. One common feature with the bright positions (2, 4, 8) is that oxygen could not be detected. Some elements were detected (Pm, Ti, Cl) which were not in the base metal. An explanation for this could be that they were introduced through the electrode. The scanning electron microscope images, optical micrographs, and energy dispersive spectroscopy (EDS) analysis for the weldment produced with an E308L -16 electrode are shown in Figure 2. A qualitative examination of the welded joint indicates that the welded joint is homogenous with few spots, which are possibly inclusions. The base metal shows that the structure is homogenous, while the heat-affected and fusion zones show the formation of uniform-sized grains.

EDS analyses were carried out on the spots with marks numbered 1 to 8 to check how the elements are distributed in the weldment. The distributions of the elements in these spots are shown in Table 5. There are more alloying elements in the stainless steel electrodes compared to the non-stainless steel electrodes, and some of these elements (chromium, titanium, nitrogen, promethium, manganese) are expected to act as ferrite stabilizers which promote ductility, toughness, crack resistance, and hardness. The welded joint should comprise 60 % of the constituents from the electrode and 40 % of the constituents from the base metal with some fractions from the environment. To maintain duplex (austenite and ferrite) phases, the weldments must meet a minimum of 17 wt. % Cr and 7 wt. % Ni. Based on this assumption, and considering the composition of the base metal and the electrode, the amount of Cr, Ni, and Mn expected in the weldments with stainless steel electrodes are approximately 17.5, 4.02, and 3.9 wt. % respectively. This is so because Ni has been replaced with Mn in the base metal. The amount of Cr, Ni, and Mn expected in the weldments with non-stainless steel electrodes are approximately 5.5, 0.24, and 4 wt. %, respectively. This result does not meet the requirement to produce ferritic-austenitic stainless steel weld metal. Still, it produces a martensitic phase with very high hardness values, making the weldments prone to stress corrosion cracking.

Table 5: Table showing the elements present at the marked spots where the EDS analyses were carried out for weldment with E308L -16 electrode

	Position on the micrograph								
Element Conc. (wt. %)	**1**	**2**	**3**	**4**	**5**	**6**	**7**	**8**	**Average**
Fe	51± 1.4	75.6±1	15.5±3.7	49.6±1.2	26.5±1.9	33.4±2.6	16±3.1	72.3±1.2	42.5±2
Cr	14.7±2	18.6±1.7	-	7.1±2.7	19.2±1.8	-	-	20.9±1.7	10±1.2
O	19.9±2.3	-	41±0.7	-	34±2	38±2.8	45.6±2.3	-	22.3±1.3
C	14.4±1.2	5.8±1.9	43.5±0.7	16.7±0.9	5.8±1.7	24.3±1.3	24.8±0.8	6.8±2	17.8±1.3
Pm	-	-	-	26.6±3	-	-	-	-	3.3±0.4
Ti	-	-	-	-	14.5±1.8	-	-	-	1.8±0.2
Cl	-	-	-	-	-	4.3±4.8	-	-	0.5±0.6

The electron micrograph of the weldment with E308L electrode, optical micrographs of the base metal, heat affected zone, fusion zone, and the microstructure of the sample showing the spots where the EDS analyses were carried out are shown in Figure 3. The grains are well formed with clear grain boundaries for the base metal, heat-affected, and fusion zones. One common feature among the three is that the grains appear to be oriented along the rolling direction of the steel. Bright and dark features are also observed in the microstructure with inclusions. To determine the elements present, the EDS is done with the analysis in Table 4. Low amounts of Cr were observed at spots 2, 3, and 8, while wholly depleted at spots 4 and 5. High-than-average concentrations of carbon were observed on positions 4, 5, and 6, while new elements (Pm, Ti, and Cl) were detected.

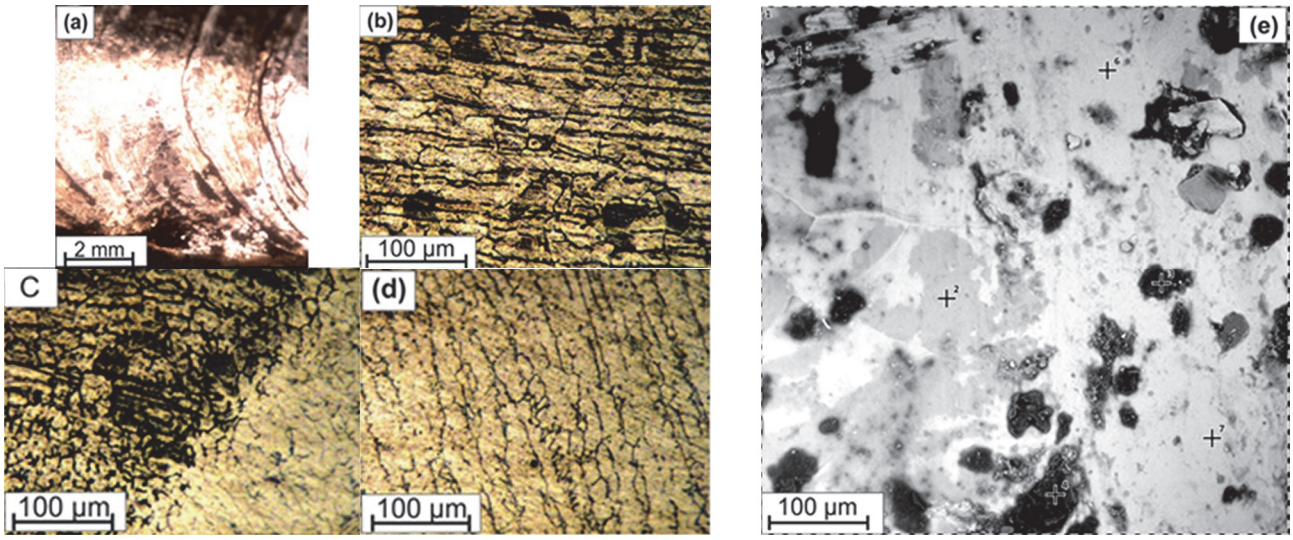

Figure 3: (a) Scanning electron micrograph of the welded joint using stainless steel E308L electrode (b) Optical micrograph of the base metal with a magnification of X200 (c) Heat Affected Zone of the 308L electrode with magnification X200 and (d) the fusion zone of the E308L electrode with magnification X200 and (e) Micrograph of the welded joint with E308L electrode showing the spots where the EDS analysis was carried out

The electron micrograph of the weldment with E6013 electrode, optical micrographs of the base metal, heat affected zone, fusion zone, and the microstructure of the sample showing the spots where the EDS analyses were carried out are shown in Figure 4.

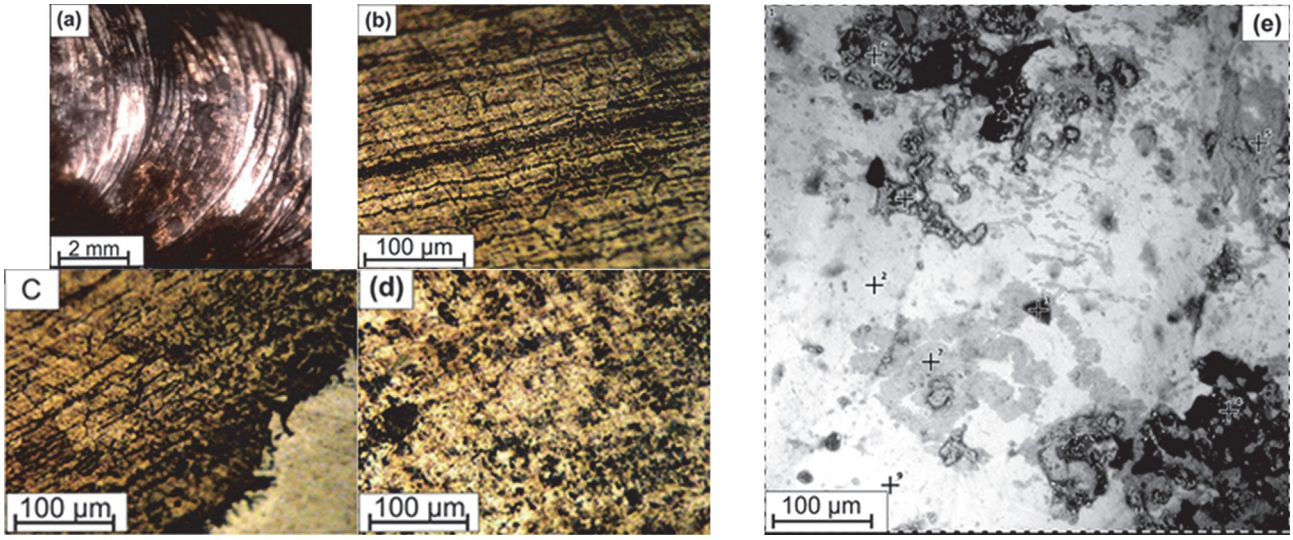

Figure 4: (a) Scanning electron micrograph of the welded joint using E6013 electrode (b) Optical micrograph of the base metal with magnification of X200 (c) Heat Affected Zone of the E6013 electrode weldment with magnification X200 and (d) the fusion zone of the E6013 electrode weldment with magnification X200 and (e) Micrograph of the welded joint with E6013 electrode showing the spots where EDS analysis was carried out.

Clearly defined grains with grain boundaries are observed on the base metal and the heat-affected zone region, but at the fusion zone, the structure needs to be clearly defined while pits and holes are observed. Bright and dark microstructural features with inclusions are observed on the microstructure of the welded sample. The EDS analysis of the micrograph is shown in Table 6. Cr was not observed, while high carbon content was observed on positions 4, 6, and 8 on the micrograph. Low contents of iron and oxygen were observed on positions 5 and 1, as well as 2 and 4, respectively. Elements like Si, Ti, and Mn were also observed and are believed to come from the base metal.

Table 6: Table showing the elements present at the marked spots where the EDS analyses were carried out for weldment with E308L electrode

	Position on the micrograph								
Element Conc. (wt. %)	**1**	**2**	**3**	**4**	**5**	**6**	**7**	**8**	**Average**
Fe	49.5± 1.5	41.1±1.4	20.8±1.8	21.3±2.8	33.7±2.8	47.9±1.5	77.6±1.3	55.2±1.3	43.4 ±1.8
Cr	17.9±1.9	7±3	7.6±2.4	-	-	18.1±2	20.1±2	8.9±2.8	9.95±1.8
O	23.2±2.2	20±2.2	35.3±1.5	54.6±1.9	37.6±3.4	17.2±3	-	-	23.5±1.8
C	4.8±2.2	4.1±2.2	1.1±3.5	16.7±0.9	11.7±2.2	13±1.3	2.4±4	1.3±4.9	6.9±2.7
Pm	-	24.1±3.5	23.7±3	26.6±3	-	-	-	34.5±3.1	13.6±1.6
Ti	4.6±4.1	3.8±4	11.5±1.7	-	14.5±1.8	3.8±4.7	-	-	4.8±2
Cl	-	-	-	-	4.9±4.7	-	-	-	0.6±0.6

The EDS analyses of the weld metals with E6013 and E7018 electrodes show a depletion of chromium content and minimal alloying elements, thereby producing more carbide precipitates and thus increasing the hardness levels of the weld metal, thereby making them martensitic and prone to stress corrosion cracking.

The electron micrograph of the weldment with E7018 electrode, optical micrographs of the base metal, heat affected zone, fusion zone, and the microstructure of the sample showing the spots where the EDS analyses were carried out are shown in Figure 5. Visual examination of the weldment reveals the presence of inclusions, while the heat-affected zone shows clearly defined grains with grain boundaries. The analysis of the weldment using EDS is shown in Table 8. Bright and dark features can be seen on the microstructure, while the grey spots appear to be a new phase. The dark spots 3 and 6 indicate that the Fe content is low. Spots 5, 6, and 7 suggest that oxygen content is low. Elements like Si, Ti, Mn, and Pm were also observed on the dark features of the micrograph.

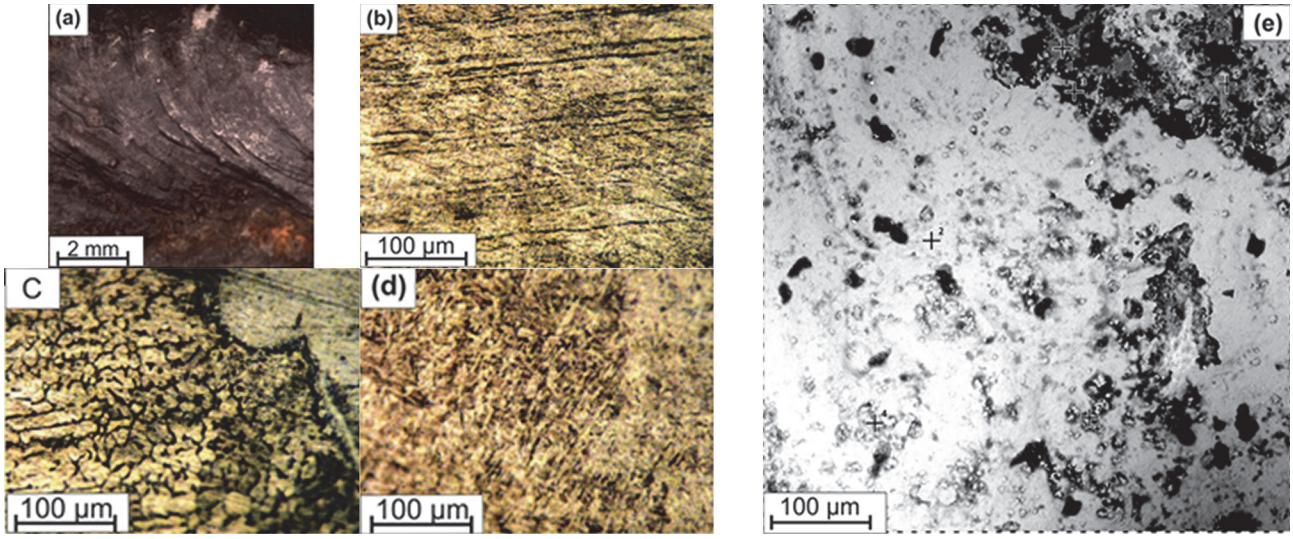

Figure 5 (a) Scanning electron micrograph of the welded joint using E7018 electrode (b) Optical micrograph of the base metal with magnification of X200 (c) Heat Affected Zone of the E7018 electrode weldment with magnification X200 and (d) the fusion zone of the E7018 electrode weldment with magnification X200 and (e) Micrograph of the welded joint with E7018 electrode showing the spots where EDS analysis was carried out

Table 7: Table showing the elements present at the marked spots where the EDS analyses were carried out for weldment with E6013 electrode

	Position on the micrograph								
Element Conc. (wt. %)	**1**	**2**	**3**	**4**	**5**	**6**	**7**	**8**	**Average**
Fe	64.8± 1.3	75.2±1.1	40.1±1.7	51.9±2.4	19±2.5	41.1±2	57.2±1.4	35.1±2.1	48±1.8
O	31.8±1.7	23.4±1.8	52.6±1.3	32.2±3.1	50.7±1.7	45.6±1.8	36.7±1.6	42.5±2	39±1.9
C	3.5±2.8	1.4±4.3	7.3±1.7	10.8±2.5	1.8±3.7	13.2±1.4	6.1±2	22.4±1	8.3±2.4
Si	-	-	-	5.1±4.6	2.9±3.7	-	-	-	1±1
Ti	-	-	-	-	14.6±2.1	3.8±4.7	-	-	2.3±0.85
Mn	-	-	-	-	11.1±3.1	-	-	-	1.4±0.4

Table 8: Table showing the elements present at the marked spots where the EDS analysis was carried out for weldment with E7018 electrode

	Position on the micrograph							
Element Conc. (wt. %)	**1**	**2**	**3**	**4**	**5**	**6**	**7**	**Average**
Fe	62.1± 1.1	66.6±0.9	22.6±1.8	58.8±1.1	79.1±1.5	14.8±2.7	78.4±1.0	54.6±1.4
O	35.2±1.3	31.8±1.2	45.4±1.3	32.2±1.4	18.8±2.8	19.8±2.5	19.5±1.9	29±1.8
C	2.7±2.5	1.7±3	3.5±2.1	3.7±2.2	2.1±4.5	13.2±1.4	2.1±3.2	4.1±2.7
Si	-	-	3.6±2.7	5.1±4.6	-	2.4±4.5	-	1.6±1.7
Ti	-	-	3.2±4	-	-	3.8±4.7	-	1±1.24
Mn	-	-	15.2±2	-	-	6.3±3.7	-	3.1±0.8
Pm	-	-	-	-	-	34.0±2.3	-	4.9±0.3

4. CONCLUSION

The effect of using different welding electrodes to weld austenitic stainless steel type 204 has been investigated in this work. It is advised that before any steel product bought without the manufacturer's data sheet is used, chemical composition analysis should be carried out to ascertain the steel type. High hardness values are obtained when non-stainless steel electrodes (E6013 and E7018) weld the austenitic stainless steel plates. The vast difference in the prop-

erties of the base metal and the welded joint introduces stresses that will eventually lead to the cracking of the material. The ultimate tensile strength and hardness values of the welds with non-stainless steel electrodes are also very high compared to those with stainless steel electrodes. However, heat treatment after the welding results in even higher hardness and ultimate tensile strength values for all the weldments except for the E6013 electrode. Heat treatment of the welded joint is, therefore, not a solution because the hardness values increase even for the welds with stainless steel electrodes. Since the carbon in the steel may react with the chromium to form chromium carbide, which is a complex but brittle phase. The microstructural examination showed that although the welded joints appear good, there are pits in the welds with non-stainless steel electrodes. The energy dispersive spectroscopy shows the non-homogenous distribution of the elements and the introduction of elements possibly from the environment. It is, therefore, advisable to use appropriate electrodes to weld austenitic stainless steel.

REFERENCES

[1] P. O. Okonji, E. E. Nnuka, and J. U. Odo, "Effect of welding current and filler metal types on macrostructure and tensile strength of GTAW welded stainless steel joints", International Journal of Scientific Research and Engineering Trends, Vol. 1(1), pp. 9-12, (2015)

[2] M. F. Buchely, H. A. Colorado, H. E. Jaramillo, "Effect of SMAW manufacturing process in high-cycle fatigue of AISI 304 base metal using AISI 308L filler metal,", Journal of Manufacturing Processes, Vol. 20(1), pp. 181-189, http://dx.doi.org/10.1016/j.jmapro.2015.08.005, (2015)

[3] "Welding of stainless steels and other joining methods", A Designers' Handbook, American Iron and Steel Institute, Washington D.C. (USA), (1988)

[4] S. Kumar and R. Singh, "Investigation of tensile properties of shielded metal arc weldments of AISI 1018 mild steel with preheating process", Materials Today: Proceedings, Vol.26(2), pp. 209-222, https://doi.org/10.1016/j.matpr.2019.10.167, (2020)

[5] B. J. Kutelu, E. G. Adubi, and S.O. Seidu, "Effects of electrode types on the microstructure, tensile and hardness properties of 304 L austenitic stainless steel heat-affected zone (HAZ)", Journal of Minerals and Materials Characterization and Engineering, Vol. 6(5), pp. 531-540, https://doi.org/10.4236/jmmce.2018.65038, (2018)

[6] N. R. Baddoo, "Stainless steel in construction: A review of research, applications, challenges and opportunities", Journal of constructional steel research, Vol. 64(11), pp. 1199-1206, http://dx.doi.org/10.1016/j.jcsr.2008.07.011, (2008)

[7] M. J. Joseph and M. A. Jabbar, "Effect of aging process on the microstructure, corrosion resistance and mechanical properties of stainless steel AISI 204", Case Studies in Construction Materials, Vol. 11, https://doi.org/10.1016/j.cscm.2019.e00253, (2019)

[8] A. M., Tahir, N. A. M. Lair, and F. J. Wei. "Investigation on mechanical properties of welded material under different types of welding filler (shielded metal arc welding)", 3rd International Conference on the Science and Engineering of Materials (ICoSEM 2017), Kuala Lumpur (Malaysia), pp. 020003-1-020003-7, Vol. 1958(1), https://doi.org/10.1063/1.5034534, (2018)

[9] A. S. Abdel-Wanees, T. S Mahmoud, and I. M Ibrahim, "Effect of electrode material on microstructural and mechanical characteristics of AISI 304 stainless steels plates joined using shielded metal arc welding", Engineering Research Journal (Shoubra), Vol. 44(1), pp. 1-4, https://doi.org/10.21608/erjsh.2020.242093, (2020)

[10] H. Vashishtha, R.V. Taiwade, R.K. Khatirkar, and A.S. Dhoble, "Effect of austenitic fillers on microstructural and mechanical properties of ultra-low nickel austenitic stainless steel", Science and Technology of Welding and Joining, Vol. 21(4), pp. 331-337, http://dx.doi.org/10.1080/13621718.2015.1112604, (2016)

[11] G. Magudeeswaran, V. Balasubramanian, T. S. Balasubramanian, and G. Madhusudhan Reddy, "Effect of welding consumables on tensile and impact properties of shielded metal arc welded high strength, quenched and tempered steel joints", Science and Technology of Welding and Joining, Vol. 13(2), pp. 97-105, http://dx.doi.org/10.1179/174329307X249432, (2008)

[12] M. Mosaad and S. S. Mohamed, "Effect of electrode type on the characteristics of AISI 316 stainless steel", Engineering Research Journal (Shoubra), Vol. 44(1), pp. 5-9, https://doi.org/10.21608/erjsh.2020.242094, (2020)

[13] A. Oyetunji, and N. Nwigboji, "Effect of welding process, type of electrode and electrode core diameter on the tensile property of 304L austenitic stainless steel", Leonardo Electronics Journal of Practices and Technologies, Vol. 13(25), pp. 210-222, (2014)

[14] F. A. Ovat, L. O. Asuquo, and A. J. Anyandi, "Microstructural effects of electrodes types on the mechanical behaviour of welded steel joints", Research Journal in Engineering and Applied Sciences, Vol. 1(3), pp. 171-176, (2012)

[15] https://www.pinnaclealloys.com